2001-01-0898

Throw Model for Frontal Pedestrian Collisions

Inhwan Han, Associate Professor
Hong Ik University, Choongnam, South Korea
Raymond M. Brach, Professor
University of Notre Dame, Notre Dame, IN, USA

ABSTRACT

A planar model for the mechanics of a vehicle-pedestrian collision is presented, analyzed and compared to experimental data. It takes into account the significant physical parameters of wrap and forward projection collisions and is suitable for solution using mathematics software or spreadsheets. Parameters related to the pedestrian and taken into account include horizontal distance traveled between primary and secondary impacts with the vehicle, launch angle, center-of-gravity height at launch, the relative forward speed of the pedestrian to the car at launch, distance from launch to a ground impact, distance from ground impact to rest and pedestrian-ground drag factor. Vehicle and roadway parameters include postimpact, constant-velocity vehicle travel distance, continued vehicle travel distance to rest with uniform deceleration and relative distance between rest positions of vehicle and pedestrian.

The model is presented in two forms. The first relates the throw distance, s_p, to the initial vehicle speed, v_{c0}, that is, $s_p = f(v_{c0})$. The second, intended for reconstruction, relates the vehicle speed, v_{c0}, to the pedestrian throw distance, s_p, that is, $v_{c0} = f(s_p)$. The first form is used extensively in the paper as means of comparison of the model to over 14 selected sets of experimental data taken from the current literature. The second form is fit to experimental data, providing values of two model parameters, A and B.

INTRODUCTION

Well over 400 technical papers have been written in the past 30, or so, years on the topic of vehicle-pedestrian accidents. A significant number of these articles present and discuss statistics of pedestrian accidents, types and trends of injuries, types, trends and categories of vehicle frontal geometries, typical vehicle deformations, etc. Others present and discuss physical and mathematical models for the analysis and reconstruction of such pedestrian accidents. The form of these models varies widely, however and ranges from statistical and/or empirical equations to relatively sophisticated mathematical mechanics models. Examples of the former are Evans & Smith (1999), Happer, et al. (2000) and Limpert (1984, 1998). Examples of the latter include the simulation models of van Wijk, et al., (1983), Moser, et al., (2000) and the momentum models of Wood, (1988). A compilation of numerous vehicle-pedestrian accident reconstruction formulas is given by Russell, (undated). A book by Eubanks (1994), gives broad coverage to pedestrian accidents including related topics such as tabulated pedestrian speeds. A compilation of technical papers representing basic studies and results is contained in a volume edited by Backaitis (1990).

This paper deals with throw distance, the distance along the road between the location of the initial pedestrian-vehicle contact and the pedestrian rest position. It deals with modeling of the relationship between throw distance and vehicle speed. Using mathematics and physics to model the throw distance presents a challenge, for several reasons. First and foremost is the fact that relative to the vehicle, the human body is articulated, flexible and soft, though the skeletal structure provides limited rigidity (but capable of fracture). For low vehicle frontal shapes, it is common to have a primary collision between the frontal portion of the vehicle (bumper, grill, etc.) and the lower

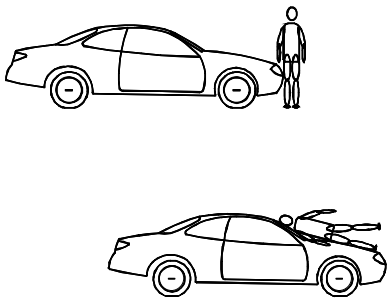

Figure 1. Diagram of primary (top) and secondary (bottom) impacts between a pedestrian and a vehicle.

part of the pedestrian followed by a secondary collision of an upper part of the pedestrian with the hood, windshield or roof as shown in Fig. 1. In low speed collisions, the secondary impact may be nonexistent or minor. Wide variations occur in human size, weight and form; wide variations exist in the size and frontal geometry of vehicles and wide variations occur in the initial conditions of contact between the two. For a given human form, size and weight and a given vehicle frontal geometry and compliance, the resulting motion of the pedestrian depends significantly on the initial speed of the vehicle. All of these effects couple since the location and severity of a secondary collision is dependent on the speed. In addition, a portion of the pedestrian's motion before coming to rest is with ground contact. Because of the articulated shape of the human body, this motion can consist of combinations of bouncing, tumbling, rolling and sliding. In fact, this type of motion has received considerable attention in its own right; for example see Bratten (1989) and Searle (1993). All of these variations are difficult to model. They also are difficult to control during experiments.

Limpert (1998) splits a vehicle-pedestrian collision into 3 phases, the impact phase, the flight phase and the sliding and/or rolling phase. Five categories of vehicle-pedestrian collisions are described by Ravani, et al., (1981), Brooks, et al. (1987) and others. These are wrap, forward projection, fender vault, roof vault and somersault collisions. A wrap collision is one where a significant portion of the pedestrian's body extends above the forward or frontal portion of the vehicle and the pedestrian's body "wraps" up onto another portion of the vehicle such as the hood (bonnet), windshield and/or roof; such as in Fig 1. Wrap contact is accompanied by a rotation and bending of the pedestrian's body and often is followed by a secondary impact of the head and/or upper torso. In a fender vault, the pedestrian falls or rolls off to the side of the moving vehicle. For a roof vault, the vehicle passes under the pedestrian as it does for a somersault, where the pedestrian goes over the roof and rotates, typically to an inverted, head-down, position.

In this paper, wrap collisions are considered to be those that have both primary and secondary collisions and a forward projection has only a primary collision. Of course, aberrations occur. An example of this category is where a pedestrian rises up onto the hood, perhaps suffers a secondary collision, and remains on the hood without being thrown forward. In cases such as these, the pedestrian typically slides from the hood either to the side or forward, depending on the braking and steering of the vehicle. In this case there is a "carry" phase between impact and flight. This is not considered in this paper. The model developed in this paper is intended to handle wrap, forward projection, roof vault and somersault collisions. Unfortunately, there seems to be no experimental data available to study the last 2 categories, so these are not treated here in any depth.

Following impact the pedestrian then is thrown forward from the vehicle and begins a flight phase, particularly if the vehicle is decelerating. A forward projection collision is usually defined for a type of collision where the pedestrian's body does not extend significantly above the forward portion of the vehicle and the initial contact drives the pedestrian directly forward into the flight phase after a single impact. In both categories, the pedestrian's center of gravity is above the ground when it departs contact with the car. The mechanics of the flight phase can be described by the equations of free flight under gravity. Ordinarily, air drag is neglected for the flight phase and is neglected here. The flight phase is followed by an impact with the ground.

The size and frontal geometry of the vehicle are factors that influence the mechanics of throw distance. Many authors have studied these aspects of collisions; for example, see Ashton and Mackay (1979), Sturtz and Suren (1976) and Evans and Smith (1999). There appears to be some disagreement on the significance of frontal geometry. On the one hand, Limpert (1998) claims that frontal geometry and the identification and measurement of the location of the secondary impact can be critical in reconstruction to the extent that small errors can result in significant differences in speed reconstruction. Yet, Evans and Smith (1999) say that the effect of frontal geometry is overrated. On balance, frontal geometry probably does play a role in vehicle-pedestrian mechanics and reconstruction but has no special significance or sensitivity. It is also likely that the vehicle frontal geometry, pedestrian height, weight and speed factors interact, or couple. For a given frontal geometry, the location and severity of the secondary impact depends on the speed and pedestrian geometry. In the model that is presented, a single variable is used to represent the distance

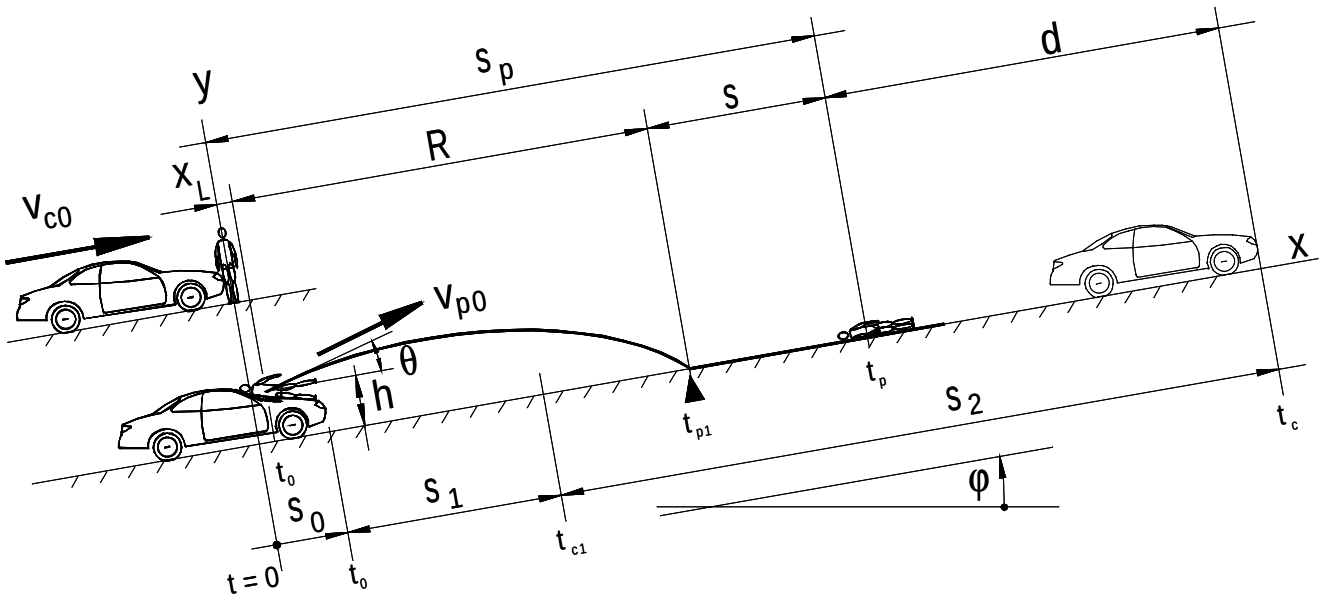

Figure 2. Coordinates, variables and events corresponding to a vehicle-pedestrian collision.

between the primary impact and the secondary impact.

A main goal of this paper is to develop a model of a vehicle-pedestrian collision that is somewhat more comprehensive than others, yet is not overly complex and remains practical and realistic. A comparison is made of the model with experimental results. This comparison is rather extensive yet not fully satisfying, for several reasons. One reason is that measurements of some of the variables included in the model (such as the range of the flight phase and slide distance) typically are not made or reported from experiments and so direct comparisons cannot be made. Other factors play a role such as the common use of dummies for experiments (for obvious reasons). The differences between results from experiments using dummies and humans often is investigated through the use of actual accidents. Actual accidents, of course, require reconstruction, a process that introduces another set of associated unknowns and variations. Wood and Simms (1999) discuss some of these issues. Another approach is to use cadavers, but the number of such experiments is limited; these results also have their own peculiarities. Part of the paper is devoted to a preliminary analysis of some of the data used in the comparisons.

Caution must always be used in the application of any mathematical model of the mechanics of vehicle-pedestrian collisions. Collisions are not ideal. A pedestrian is not a rigid body, contact often occurs between the pedestrian and vehicle during the early part of the flight phase, motion along the ground is combination of sliding, rolling & tumbling, not simply sliding, etc. Consequently, wide variations can be expected between theory and practice. And, in fact, wide variations occur in experiments. This must be taken into account. A concerted study of the case-to-case variations from the model is not made in this paper since many of the variables in the model remain unmeasured; more experimental work needs to be done. Confidence limits have been studied by other authors such as Evans & Smith (1999) and Happer, et al. (2000). Typically these limits are broad and may not apply directly to a particular data set or to a specific application of a model.

A simplified pedestrian collision index model is presented. A purpose for the collision index model is that it can be used to help interpret experimental data. It also is compared to the paper's model in predicting pedestrian collision mechanics.

PEDESTRIAN IMPACT MODEL

THROW DISTANCE MODEL

Figure 2 shows a diagram that illustrates coordinates, parameters and some of the events of a vehicle-pedestrian collision. An objective is to determine the total throw distance, s_p, as a function of the initial vehicle speed, v_{c0}, with all of the other quantities (such as launch angle, θ, launch height, h, road grade, φ, etc.) treated as known parameters. Another objective is to model the motion of the vehicle and relate it to the pedestrian throw distance.

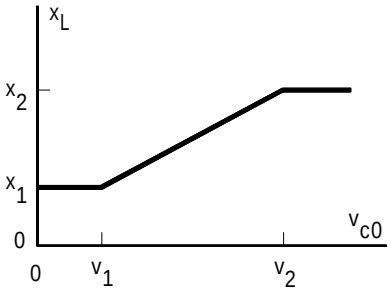

Figure 3. Sample relationship between x_L and the initial vehicle speed.

The throw distance can be written as:

$$s_p = x_L + R + s \tag{1}$$

where x_L is the distance the pedestrian moves in the time between the primary and secondary impacts. The parameter x_L is included to represent the combined influence of the vehicle frontal geometry, pedestrian center-of-gravity height at impact, and vehicle speed dependence of the secondary impact. R is the range, or ground distance, covered during the flight phase and s is the distance between the ground impact of the pedestrian and the rest position. Some analysts, such as Limpert (1998), represent the initial velocity of the pedestrian, v_{p0}, as a fraction or multiple of the forward speed of the vehicle. For that reason (and to allow comparisons of this concept with experimental results) the initial launch speed of the pedestrian, v_{p0}, is expressed as

$$v_{p0} = \alpha v'_{c0} \tag{2}$$

where α is a constant and v'_{c0} is the speed of the car at the time the pedestrian is launched. The pedestrian is launched following the secondary collision, or the primary, if no secondary collision takes place. Between initial contact and launch, the pedestrian is brought up to speed and the vehicle suffers a momentum loss. Based on conservation of momentum,

$$v'_{c0} = \frac{m_c}{m_c + m_p} v_{c0} \tag{3}$$

where v_{c0} is the speed of the vehicle at initial contact, m_c is the mass of the vehicle and m_p is the mass of the pedestrian. The range, R can be expressed as

$$R = v_{p0} \cos\theta \, t_R - g \sin\varphi \, t_R^{\,2} / 2 \tag{4}$$

The quantity t_R is the flight time from launch to ground contact and is

$$t_R = \frac{v_{p0} \sin\theta}{g \cos\varphi} + \frac{\sqrt{v_{p0}^2 \sin\theta + 2gh\cos\varphi}}{g\cos\varphi} \tag{5}$$

The velocity components of the pedestrian at the time of ground impact are:

$$v_{pRx} = v_{p0} \cos\theta - g \sin\varphi \, t_R \tag{6}$$

and

$$v_{pRy} = v_{p0} \sin\theta - g \cos\varphi \, t_R \tag{7}$$

These last two velocity components are velocity components just as the pedestrian impacts the ground. Following impact, vertical rebound is possible, even bouncing is possible. However, it can be shown that the horizontal travel distance is not highly dependent on multiple bouncing. Consequently, it is assumed that there is a single impact normal to the ground and that it is perfectly inelastic, so the postimpact rebound velocity is

$$v'_{pRy} = 0 \tag{8}$$

Further, it is assumed that Coulomb friction acts during the impact with the ground so the tangential component of the postimpact velocity is given by:

$$v'_{pRx} = v_{pRx} + \mu \, v_{pRy} \tag{9}$$

The quantity, μ, is the ratio of the tangential impulse to the normal impulse during the impact. Throughout this paper, the pedestrian sliding drag factor is used for μ. Note that v_{pRy} is negative so that $v'_{pRx} < v_{pRx}$. The final part of the throw distance is the slide distance, s. This is calculated using a pedestrian drag factor, f_p where:

$$s = \frac{\left(v'_{pRx}\right)^2}{2g\left(f_p \cos\varphi + \sin\varphi\right)} \tag{10}$$

The model for pedestrian throw distance now is complete where $s_p = f(v_c)$ is given by using Eq 4 and 10 with Eq 1.

Modeling of x_L It was mentioned above that x_L represents the distance the pedestrian (center of gravity) travels in the time between the initial and secondary impacts with the vehicle. In tests with dummies, Kallieris and Schmidt (1988) found that the location of the secondary impact depends on the speed of the car. Similar results were found by van Wijk, et al., (1983) from reconstructed accidents. In the following, a bilinear function is used to represent this distance as it varies with vehicle speed. Figure 3 shows the function where the values, x_1 = 0.5 m (1.6 ft), x_2 = 1.5 m (4.9 ft), v_1 = 5 m/s (11 mph) and v_2 = 20 m/s (45 mph) are used in this paper. By definition, x_L = 0 for forward projection collisions. To some extent, the nonlinear function in Fig 3 is arbitrary and requires experimental verification but it does allow roof vaults and somersaults to be modeled.

VEHICLE MOTION

Vehicle motion exists simultaneously with the pedestrian motion and is separated into 3 portions. The first is a distance, s_0. As a rough approximation, it is assumed that over the distance, x_L, the pedestrian

travels at half its launch velocity so, $t_0 \approx x_L/(v'_{c0}/2)$ and $s_0 \approx v_{c0}\, t_0$. Next, the vehicle can travel a distance, s_1, at constant velocity and finally a subsequent portion of the motion, s_2, with constant deceleration, a_2. Of course, s_1 can be zero if deceleration exists from t_0 to rest. Consequently,

$$\begin{aligned} d &= s_0 + s_1 + s_2 - s_p \\ d &= v_{c0}t_0 + v'_{c0}(t_{c1} - t_0) + \\ &\quad a_2(t_c - t_{c1})^2 / 2 - s_p \end{aligned} \tag{11}$$

THROW DISTANCE INDEX

Evans & Smith (1999) and Happer, et al. (2000), use curve fitting techniques to arrive at a relationship between the throw distance, s_p, and the initial vehicle speed, v_{c0}. A modified form of their relationship is:

$$s_p = c_1(v_{c0} + c_2)^2 \tag{12}$$

For wrap collisions, Evans & Smith choose $c_2 = 0$ and find (by fitting Eq 12 to specific experimental data) that $c_1 = 1/3.58^2$ s^2/m. Happer, et al., find values of $c_1 = 1/3.53^2$ s^2/m and $c_2 = 0.72$ m/s for wrap collisions by fitting to a wide range of experimental data. As a means for comparison of experimental data sets later in this paper, a throw distance drag index is defined by an equation as Eq 12 with $c_2 = 0$, representing equivalent constant acceleration motion:

$$f_{eq} = \frac{v^2_{c0}}{2g\, s_p} \tag{13}$$

Note that f_{eq} is an equivalent constant drag factor corresponding to the entire throw distance, s_p, and not just the distance, s, when the pedestrian is in contact with the ground. The quantity f_{eq} corresponds to a fictitious, average deceleration factor for the throw distance process from impact to rest.

RECONSTRUCTION THROW MODEL

If the road grade angle, φ, is close to zero, $\varphi \approx 0$, the pedestrian throw-distance model derived above (given by Eq 4, 10 and Eq 1) can be put into a form more useful for reconstruction of the speed of the vehicle. Doing this, an equation for the initial launch speed of the pedestrian, v_{p0}, is:

$$v_{p0} = A_p\sqrt{s_p - B} \tag{14}$$

where

$$A_p = \sqrt{\frac{2 f_p g}{f_p^2 \sin^2\theta + f_p \sin 2\theta + \cos^2\theta}} \tag{15}$$

and

$$B = x_L + f_p h \tag{16}$$

Using Eq 2, 3 and 14, the velocity of the car can be expressed as:

$$v_{c0} = A\sqrt{s_p - B} \tag{17}$$

where

$$A = A_p \frac{m_c + m_p}{\alpha m_c} \tag{18}$$

With the exception that $\varphi \approx 0$, this model is a true inverse of the above throw-distance model. Recall that Eq 12, solved for the velocity v_{c0}, also is an equation used for reconstruction. Equations 17 and 12 have subtle, but important differences. First, since it is derived analytically not empirically, the parameters contained in A and B have physical interpretation, making Eq 17 more meaningful as well as more flexible. Admittedly, the values of the parameters in A and B are not always easy to estimate for specific reconstructions. Another difference between Eq 17 and 12 concerns their form. Eq 12 has an offset in the velocity whereas Eq 17 has an offset in the throw distance. Later, it will be seen that a deficiency with the throw distance index, Eq 13, is that at low velocities, it tends to underestimate the throw distance. Allowing a shift in the s_p coordinate permits better matching of experimental results.

The method of least squares was used to find values of A and B that fit the model to experimental data. This will be discussed later in more detail.

EXPERIMENTAL DATA

PEDESTRIAN DRAG FACTORS

Experimental Values of Hill The above pedestrian-impact model involves a calculation using the impulse ratio, μ, on the coefficient of pedestrian-ground friction (pedestrian drag factor) as it strikes and momentarily slides along the road surface. This parameter has not been measured for pedestrians. Experimental data are therefore needed. Hill performed a number of staged experiments designed to measure the coefficient of friction from impact to rest. He used an adult size dummy constructed using a leather suit stuffed with a mixture of sand and sawdust contained in bags. The dummy was dressed in 5 types of clothing, and in each

test, the dummy was held, face up, horizontal to and approximately 0.1m above the ground. It was released from the rear of a vehicle. The speed at release and the distance traveled by the dummy along the road between first contact and rest were measured. The pavement in all tests was a dry, airfield tarmac.

Hill used the following equation to calculate the coefficient of friction from his test results.

$$f_p = \frac{v_{p0}^{\ 2}}{2gs} \tag{19}$$

Hill found a coefficient for body to road surface of 0.8, on average, to adequately represent his test results and he used that value for calculation of vehicle speed from pedestrian throw in actual accidents.

Correction for Impact

However, Eq 19 does not take account of the effect caused by the vertical impact which occurs when the dummy strikes the road surface. The impact may be a significant event that must be accounted for when calculating the coefficient of friction.

Assuming zero road grade, Eq 20 can be obtained from Eq 8 through 10 (where $\mu = f_p$),

$$s = \frac{1}{2 f_p g}\left[v_{p0}\cos\theta - f_p\sqrt{v^2{}_{p0}\sin^2\theta + 2gh}\right]^2 \tag{20}$$

Solving for f_p gives the following equation that provides the friction drag from the test results for a zero launch-angle (Hill's conditions).

$$f_p = \left[gs + v_{p0}\sqrt{2gh} - \sqrt{(gs + v_{p0}\sqrt{2gh})^2 - 2v_{p0}^2 gh}\right] / 2gh \tag{21}$$

Note that the measured distance in the tests is the sliding and/or rolling distance s, and does not include flight range R.

From Hill's tests, Eq 21 yields an average value of friction drag of 0.74, less than 0.80 obtained by Hill. This shows that failure to account for the vertical impact with the ground results in a coefficient that is too high. The impact is a significant event that must be taken into account when calculating the coefficient of friction.

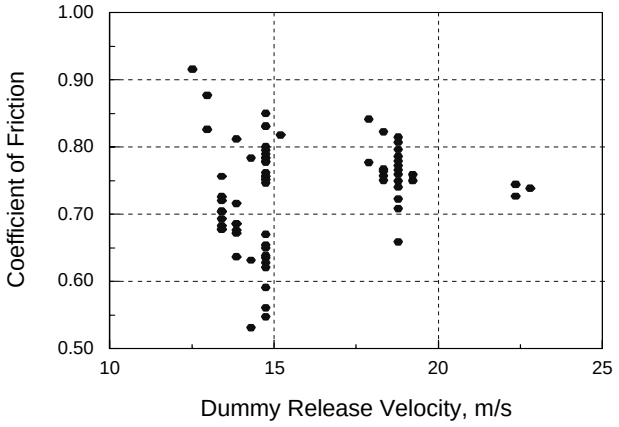

Figure 4. Coefficient of friction as a function of velocity; values calculated from Hill's data, corrected for impact.

Figure 4 shows the coefficients of friction calculated using Eq 21 plotted as a function of the horizontal release velocity for Hill's tests. Though the scatter in the data appears to vary with velocity, there seems to be no discernable trend between the releasing velocity and the coefficient of friction.

Dummy Clothing Dependence In Hill's tests, the dummy was dressed in 5 types of clothing, and a minimum of ten tests completed with each. The friction drag values show an influence of the clothing type. Through the statistical method called Analysis of Variance (ANOVA), it was concluded that the differences in values of friction drag from clothing to clothing are statistically significant. This suggests that the coefficient of friction depends on clothing. Values of f_p for the different types of clothing had a range of $0.73 \le f_p \le 0.78$ except for nylon which had an average value of $f_p = 0.61$. So although values are statistically different, only nylon showed a meaningful change.

Wood and Simms (2000) carried out a similar analysis of the data of Hill (and others). Accounting for the impact gave average values of 0.702 and 0.734 for the coefficient f using Hill's data.

EXPERIMENTAL THROW DATA

In their 2000 SAE paper, Happer, et al., presented an extensive compilation of experimental data collected from vehicle-pedestrian experiments. Some of the collection is used in this paper after grouping into to 3 categories. The first corresponds to actual accidents with adult pedestrians, where corresponding values of

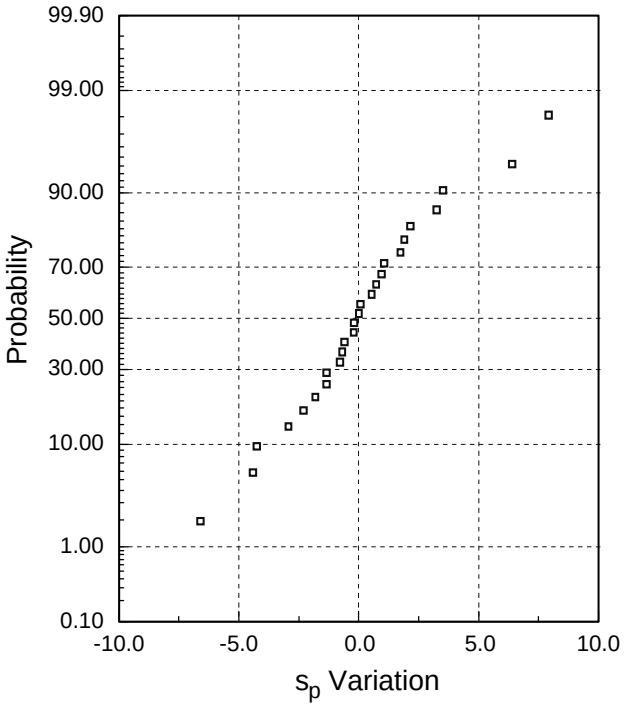

Figure 5. Normal probability plot of the deviations of Hill's measured throw distance values from the throw distance index curve.

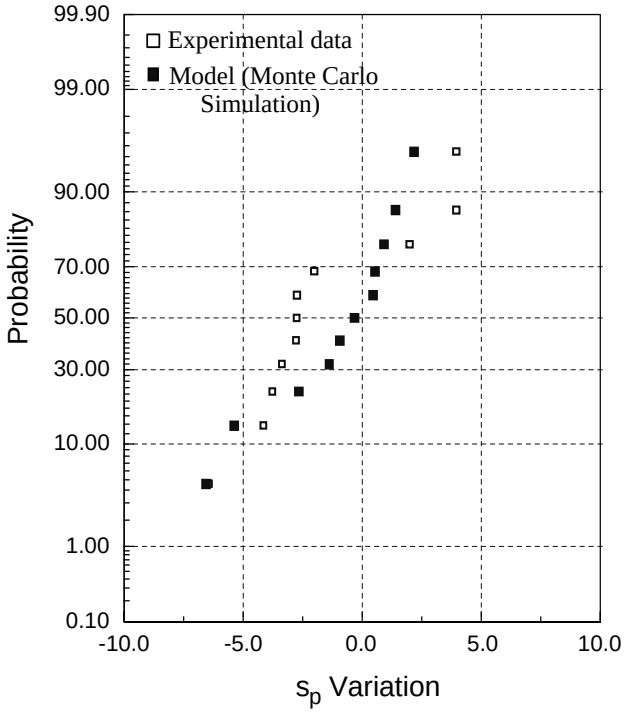

Figure 6. Normal probability plot of the deviations of Schneider's measured throw distance values from the throw distance index curve and deviations between the throw distance index curve and values from a Monte Carlo random sample of the model.

v_{c0} and s_p are obtained through reconstruction of the accidents. These include data from Dettinger (1997), Hill (1994), Kramer (1975) and Sturtz (1976). The next category corresponds to wrap trajectory collisions with adult sized dummies where s_p and v_{c0} are measured directly. These data came from Kramer (1975), Kuhnel (1974), Lucchini, et al. (1980), Schneider and Beier (1974), Severy (1966), Stcherbatcheff, et al. (1975) and Wood (1988). The final category used child sized dummies with relatively high vehicle fronts so that the collisions all were forward projection types. These data are from Lucchini, et al. (1980), Severy (1966) and Sturtz (1976).

Preliminary Analysis of Experimental Data A value of f_{eq} corresponding to each data set was calculated by minimizing the sum of squares of deviations of each data point from the index curve given by Eq 13. If Eq 13 were an exact model, then the deviations of the experimental values from the curve (sometimes referred to as *residuals*) should behave as normally (Gaussian) distributed, random experimental "error" and should plot as a straight line on normal probability paper. Furthermore, the deviations should have a mean of zero and a small standard deviation. A plot of the throw-distance deviations of Hill's data from Eq 13 is shown in Fig 5. The points lie roughly along a curve, antisymmetric about zero. This implies a narrow, symmetric distribution with wide tails, but close to normal. The mean (50% probability point) is 0.11 m and the standard deviation is 3.12 m. Unfortunately, not all data sets have such nice characteristics. Figure 6, using Schneider's data (open squares), is more typical of those showing possible "non-normal" behavior. These deviations are biased with a mean of -1.64 m and have a standard deviation of 3.42 m. Moreover, the points do not have a straight line trend. For comparison, a random sample of 11 points was generated using a Monte Carlo simulation of the model equation. These points also are plotted in Figure 6. Two parameters were given normal distributions, $N(\nu,\sigma)$, where ν is the mean and σ is the standard deviation. The statistical distributions used in the Monte-Carlo simulation are $fp = N(0.80, 0.20)$ and $\theta = N(4.21, 0.80)$. The sample points of the model more closely follow a straight line, reflecting the normality of the distributions. The apparent non-normality of the experimental variations cannot be explained but must be either from experimental events not observed and/or reported or from effects not included in the model.

Table 1. Default values of Model Parameters

α, velocity ratio, 1.0
θ, launch angle, 0° (forward projection)
φ, road grade angle, 0°
μ, pedestrian-ground impact impulse ratio, f_p
a_2, deceleration of vehicle, 0.5
f_p, pedestrian-ground drag factor, $0.7 \le f_p \le 0.8$
h, pedestrian cg height at launch, 1 m (adult), 0.4 m (child, forward projection)
m_c, mass of vehicle, 1125 kg
m_p, mass of pedestrian, 65 kg (adult) and 30 kg (child)
x_L, pedestrian displacement from primary to secondary vehicle impacts, 0 m (forward projection), Fig 3, (wrap)

With no experimental error and an exact model all deviations between them would be zero. So the better the model and the more tightly controlled the experiments, the closer the points pass through 50%, 0 and the more vertically they will be aligned (small variations). Since one of the measured variables, v_{c0}, appears to a power 2 in Eq 13, deviations may not lie along a straight line. According to statistical theory, in such a case deviations may have a distribution other than normal. Deviations of all data sets were examined and most of the probability plots showed some bias; Fig 6 is one of the "least normal". Variations of few data exhibited normality and there seemed to be no single discernable common trend.

COMPARISON OF MODEL WITH DATA

The process of fitting the model to the data sets was done in a consistent fashion. Selected parameter values were found using the method of least squares. Except for those parameter values found by curve fitting, default values were used. These are listed in Table 1. In all cases the impulse ratio, μ, representing the friction at ground impact was chosen to equal the pedestrian drag factor, f_p, that is, $\mu \equiv f_p$. This was done since there is no information on which to establish any other value of μ. Model parameters that could have been fit include h, x_L, f_p, α and θ. When experimental values of these were unknown, they were assigned "typical" values and held fixed. So, for example, h = 1 m for adult tests and 0.4 m for children (forward projection). For wrap collisions, x_L was modeled as shown in Fig 3. In wrap collisions, α was held fixed at $\alpha = 1$ and f_p and θ were found by the fitting procedure. For the forward projection cases, the launch angle was held fixed at $\theta = 0°$ and values of f_p and α were found by the fitting procedure.

The method of least squares was used to fit the model. The quantity Q was minimized, where

$$Q(u,v) = \sum_n \left[s_{pm}(u,v) - s_{pe} \right]^2 \qquad (22)$$

where u and v represent the fitted parameters, n indicates summation over all n values in a particular data set, m indicates model value of s_p and e indicates an experimental value of s_p. In the wrap experiments, $Q(u,v) = Q(f_p,\theta)$; in the forward projection cases, $Q(u,v) = Q(f_p,\alpha)$. Initially the fitting process was found to yield spurious values and so the Q(u,v) surfaces were examined. It turned out that each Q surface formed a trough in (u,v) space and the minimum would jump from one place to another along the trough. This is because a change in θ, for example, can be compensated to some extent by a change in f_p, forming a very shallow minimum. The same sort of behavior held for forward projection data. Because of this behavior, it was necessary to constrain f_p. In all cases f_p was constrained to lie between 0.7 and 0.8. These

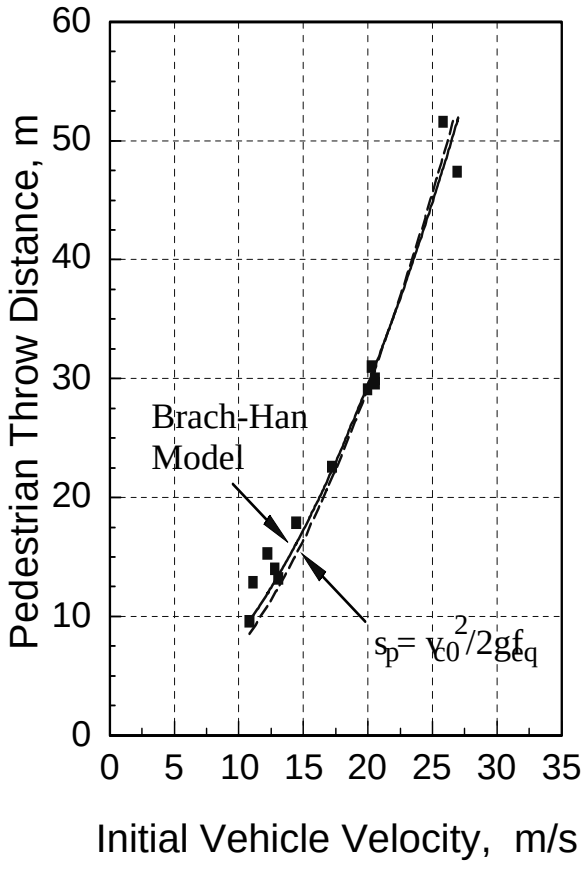

Figure 7. Dettinger's measured throw distance, the throw distance index curve and the Brach-Han model curve.

Table 2: Results of Fitting* Brach-Han Model

Source of Data	Experimental Conditions	f_{eq}	f_p	θ	α	h	$v_{c0} = f(s_p)$ Model A	$v_{c0} = f(s_p)$ Model B
Dettinger	adult/reconstruction	**0.70**	**0.8**	**7.3°**	1.0	1.0	**3.83**	**2.05**
Hill	adult/reconstruction	**0.64**	**0.7**	**5.4°**	1.0	1.0	**3.70**	**1.86**
Kramer	adult/reconstruction	**0.65**	**0.8**	**5.8°**	1.0	1.0	**3.89**	**1.66**
Sturtz	adult/reconstruction	**0.68**	**0.8**	**5.0°**	1.0	1.0	**3.93**	**1.68**
Kramer	adult/dummy/wrap	**0.60**	**0.7**	**5.2°**	1.0	1.0	**3.70**	**1.52**
Kuhnel	adult/dummy/wrap	**0.68**	**0.8**	**4.5°**	1.0	1.0	**3.95**	**1.79**
Lucchini	adult/dummy/wrap	**0.59**	**0.8**	**13.1°**	1.0	1.0	**3.63**	**1.76**
Schneider	adult/dummy/wrap	**0.74**	**0.8**	**4.2°**	1.0	1.0	**3.97**	**1.97**
Severy	adult/dummy/wrap	**0.63**	**0.8**	**9.7°**	1.0	1.0	**3.74**	**1.80**
Stcherbatcheff	adult/dummy/wrap	**0.42**	**0.7**	**35.0°**	1.0	1.0	**3.21**	**1.38**
Wood	adult/dummy/wrap	**0.50**	**0.7**	**24.9°**	1.0	1.0	**3.26**	**1.83**
Lucchini	child/forward projection	**0.46**	**0.8**	0.0°	**1.3**	0.4	**3.04**	**0.32**
Severy	child/forward projection	**0.57**	**0.8**	0.0°	**1.2**	0.4	**3.37**	**0.32**
Sturtz	child/forward projection	**0.55**	**0.8**	0.0°	**1.2**	0.4	**3.30**	**0.32**

* Values in bold type are from fitting the models to the corresponding experimental data; others are default values.

particular values were chosen for two reasons. First, from a physical standpoint, because of the presence of the flight phase (with essentially no drag), f_p must be greater than f_{eq}. With few exceptions, values of f_{eq} were found to be greater than 0.6 (see Table 2). Secondly, Hill's measurements indicate a mean value of 0.74.

Reconstructed Wrap Collisions Figures 7 and 8 show 2 of the 4 data sets of adult/reconstructed, wrap collisions with both the least-square index and model curves. Data in Fig 7 are from Dettinger data and Fig 8 from Sturtz. The model curves fit the data slightly better. The experimental points in Fig 7 show a much smaller deviation (scatter) from both curves; Fig 8 is one of the data sets with high scatter.

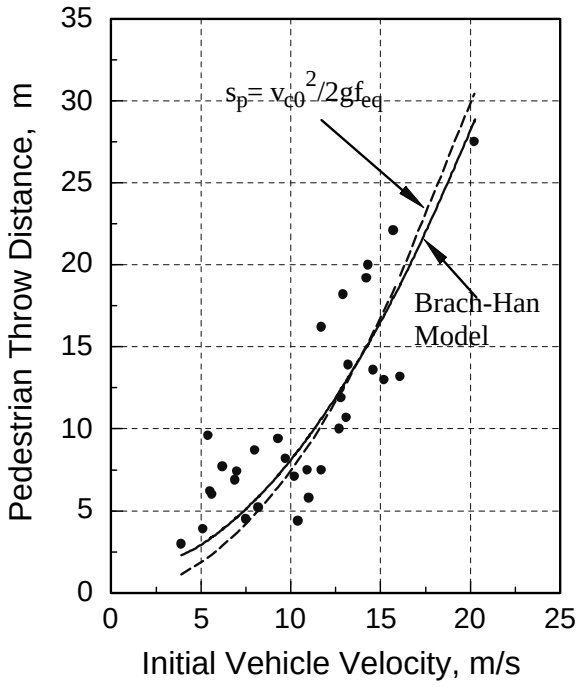

Figure 8. Sturtz's measured throw distance, the throw distance index curve and the Brach-Han model curve.

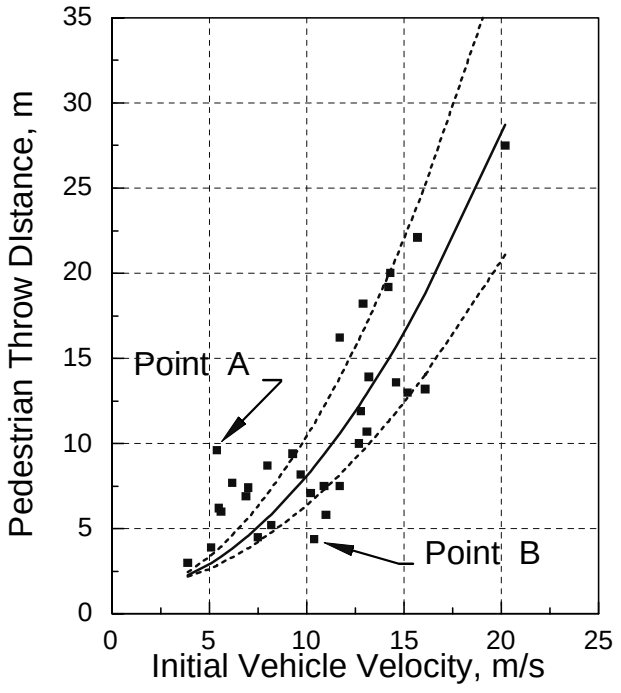

Figure 9. Sturtz's measured throw distance compared to different Brach-Han model results.

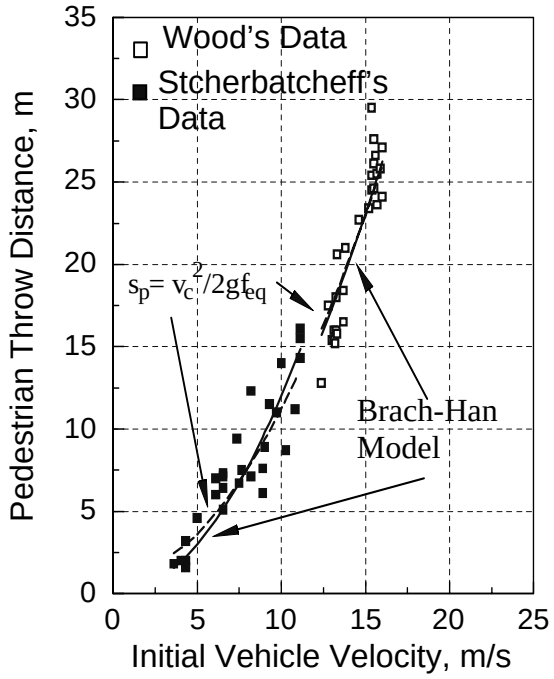

Figure 10. Measured throw distances of Wood and Stcherbatcheff, the throw distance index curves and the Brach-Han model curves.

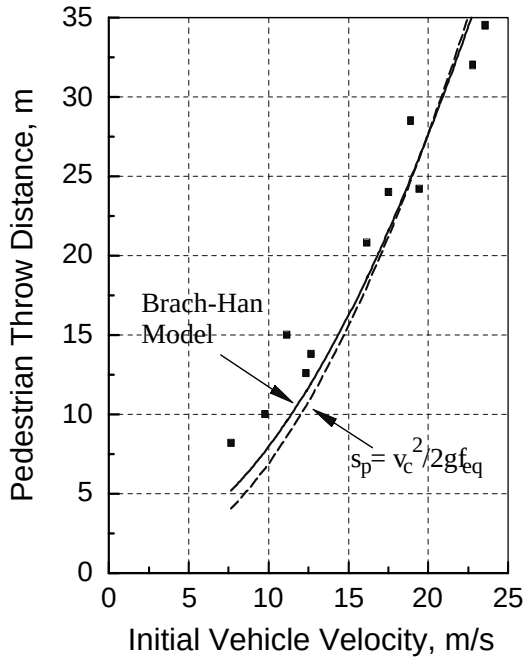

Figure 11. Schneider's measured throw distance, the throw distance index curve and the Brach-Han model curve.

Table 2 contains the results of fitting of all of the selected data sets. For adult/reconstructed wrap collisions, the equivalent drag coefficients ranged between 0.64 and 0.70. In all reconstructed wrap collisions cases, the fitting procedure gave values of f_p at the constraint boundaries and gave (unconstrained) launch angles between 5.0˚ and 7.3˚.

Figure 9 shows 3 model curves fit to the adult/reconstruction data of Sturtz. These illustrate the sensitivity of the model to the fitted values. The least-squares model curve is the solid line. Upper and lower dashed curves represent the result of arbitrary changes of θ and f_p. The upper dashed curve is for the default values and for $\theta = 10^\circ$ and $f_p = 0.2$ while the lower dashed curve is for $\theta = 0^\circ$ and $f_p = 1.0$. Not all of the experimental points are included between the dashed curves. This is not because of a lack of flexibility of the model, however. Each of the points can be fit exactly. For example, with all default values, the measured throw distance of Point A is given exactly for $\theta = -10^\circ$ and $f_p = 1.26$. Point B is matched by $\theta = -15^\circ$ and $f_p = 0.15$. Unfortunately, there is no way to know if these parameter values are realistic for these experiments. Points A and B seem unusually high and low, respectively.

Adult Dummy Wrap Collisions This type of collision had many more data sets available; seven were used in the fitting procedure. Table 2 shows the results. In all cases, fitted values of f_p were at a constraint boundary. Stcherbatcheff's and Wood's experiments gave noticeably low values of the drag index. In addition, fitting to the model produced high values of launch angle, namely $\theta = 35.0^\circ$ and $\theta = 24.9^\circ$, respectively. Their data and the fitted curves are shown in Fig 10. Underlying reasons for the differences of the launch angles of Stcherbatcheff and Wood and the rest of the cases are not known, except to say that, for given vehicle velocities, the corresponding throw distances were larger than the other data sets. Arbitrarily omitting Stcherbatcheff and Wood, the average value of launch angle for wrap collisions is 7.3˚. This compares reasonably well with the average value of $\theta = 5.9^\circ$ from the adult/reconstructed experiments.

Figure 11 shows Schneider's data. This is the data whose statistical distribution of deviations is plotted in Fig 5. Neither the model nor the throw distance index curve could be forced up high enough by the fitting procedure and so 9 of the 12 points lie above the curve (note, 2 point have the same values). This is what causes the high bias in the mean value of the

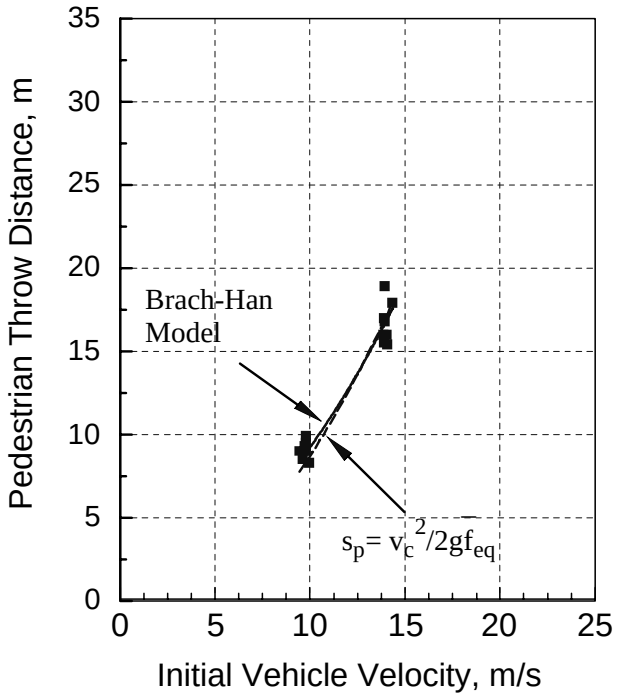

Figure 12. Lucchini's measured forward projection throw distances, the throw distance index curve and the Brach-Han model curve.

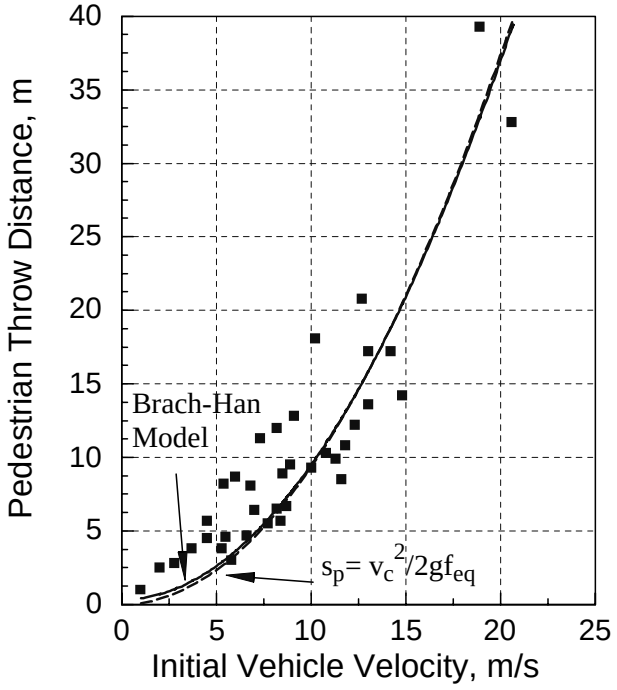

Figure 13. Sturtz's measured forward projection throw distances, the throw distance index curve and the Brach-Han model curve.

deviations seen in Fig 6. Whether this reflects a problem with the experiments or a deficiency in the models is not known.

Forward Projection Collisions Three sets of data were used in this comparison, all done with child-sized dummies and high-front vehicles. Data are from Lucchini (1980), Severy (1966) and Sturtz (1986). Fitting was done for a fixed launch angle of $\theta = 0^\circ$. The dummies had an unknown center-of-gravity height so a nominal value of 0.4 m was used. In addition, the distance x_L was fixed at 0. The least-square fitting procedure was used to find values of α and f_p (where $0.7 \le f_p \le 0.8$). Fitting of Eq 13 to find f_{eq} provided values of f_{eq} = 0.46, 0.57 and 0.55 for the Lucchini, Severy and Sturtz data, respectively. The data sets all were quite different. Figures 12 and 13 show the fitted results and data of Lucchini and Sturtz, respectively. Lucchini's data is concentrated near 2 velocity values with little scatter whereas the Sturtz data, with considerably more scatter, covers a much wider velocity range. Both the index curves and the model curves are very close for all 3 forward projection data sets.

A somewhat surprising and interesting result from these cases is that the fitted value of the velocity ratio, α,

Table 3: Results of Fitting* the Reconstruction Model, Eq 13
Experimental

Data	Conditions	A	B
Source	**Type**		
Dettinger	adult/reconstruction	3.88	3.13
Hill	adult/reconstruction	3.65	0.67
Kramer	adult/reconstruction	3.65	0.79
Sturtz	adult/reconstruction	3.71	1.20
Kramer	adult/dummy/wrap	3.48	0.31
Kuhnel	adult/dummy/wrap	3.52	0.00
Lucchini	adult/dummy/wrap	3.58	1.55
Schneider	adult/dummy/wrap	3.84	3.61
Severy	adult/dummy/wrap	3.15	0.00
Stcherbatcheff	adult/dummy/wrap	2.81	0.00
Wood	adult/dummy/wrap	3.14	0.00
Collision Type			
Adult: reconstructions & dummies		3.33	0.40
Child: reconstructions & dummies		3.24	0.74
Adult/Reconstruction		3.55	0.60
Adult/Dummy		3.21	0.24
Child/Reconstruction		3.28	0.87
Child/Dummy		3.16	0.20
Reconstruction: adult & child		3.52	0.94
Dummy: adult & child		3.20	0.25

* The coefficients A and B were found by fitting the data directly to Eq 17

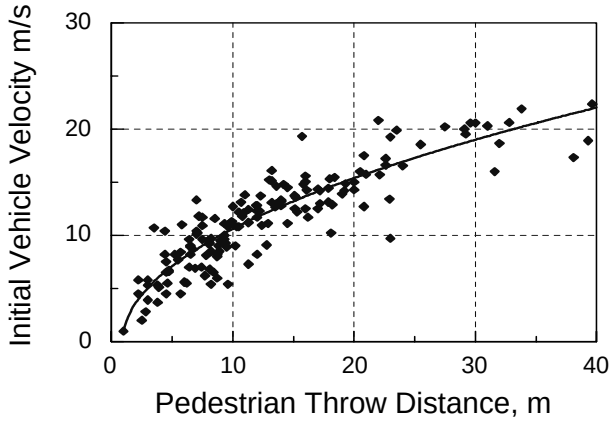

Figure 14. Model parameters A and B fitted to reconstructed collision data.

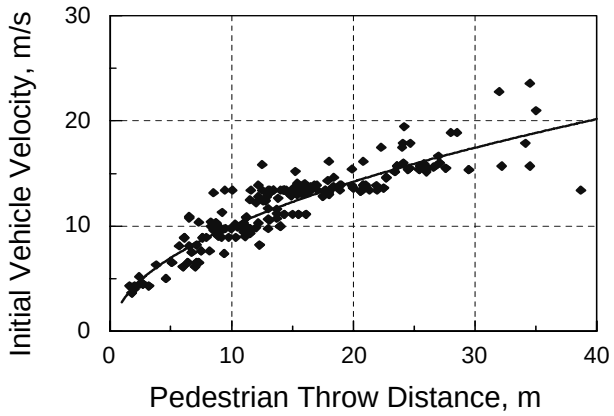

Figure 15. Model parameters A and B fitted to dummy collision data.

ranges from 1.2 to 1.3. This means that the best fit to the data is for a pedestrian forward launch velocity about 1.2 to 1.3 times greater than the forward velocity of the vehicle. The velocity loss of the vehicle due to the primary impact can be ignored here (child-to-vehicle mass ratio used here is 30/1125), so the ratio, α, corresponds to a coefficient of restitution of the primary (and only) impact. Therefore, the data indicate that in forward projection collisions, the pedestrian rebounds from the vehicle at a speed about 20% to 30% higher than the vehicle. All experiments used dummies and it is not clear if this phenomenon differs for humans, but the effect is consistent and significant.

Roof Vault & Somersault Collisions These collisions are not discussed here to any great extent since there seems to be no experimental data available. For these collisions it is expected that x_L typically would be larger than for corresponding wrap collisions. The launch angle, θ, could be expected to take on values near or greater than 90˚ and the factor α could very well be less than 1.

Fitting of the Reconstruction Model The quantity Q (u, v) again was minimized, but where

$$Q(u,v) = \sum_n \left[v_{c0m}(u,v) - v_{c0e} \right]^2 \qquad (23)$$

where n indicates summation over all n values in a particular data set, m indicates *model* value of v_{c0} and e indicates an *experimental* value of v_{c0} and (u,v) = (A,B), Eq 17. This fitting was done without any constraints. Table 3 summarizes the results. Figure 14 shows a single curve with A = 3.52 and B = 0.94 plotted with collective adult/child/reconstruction data. Figure 15 shows a single curve with A = 3.20 and B = 0.25 plotted with collective adult/dummy data.

Comparison of the values of A and B in Table 2 to those in Table 3 illustrates an extremely important difference between fitting of empirical and physical models. The fitting process of EQ 17 done to reach the values listed in Table 3 was unconstrained and, in effect, no different than finding the constants c_1 and c_2 in Eq 12. Consider the implications of one of an example pair of values of A and B from Table 3. For the data of Kramer, adult/dummy/wrap, A = 3.48 and B = 0.31. Also note that from Eq 16,

$$f_p = (B - x_L)/h \qquad (24)$$

If, for the experiments, the "average" value of the distance, x_L is about 1.0 m and the average cg height at beginning of launch is about 1.0 m, then the corresponding value of pedestrian-ground frictional drag from Eq 24 is f_p = -0.69. This certainly does not make physical sense. This demonstrates why fitting of the throw model earlier in the paper was done to physical constants. It also indicates why using a constraint was necessary when fitting the drag factor, f_p.

A comprehensive comparison of the reconstruction model with constrained comparisons with experimental data and with results of other mathematical models is planned for a separate paper.

DISCUSSION AND CONCLUSIONS

An analysis, including a correction for impact effects, of Hill's direct measurements of pedestrian-ground friction yields an average value of 0.74 and indicates that values between 0.7 and 0.8 are appropriate for f_p (for

an asphalt surface). Values of f_p greater than 0.7 also are expected since fitted values of the overall throw distance drag factor, f_{eq}, are as high as 0.70 and 0.74. These results are in contrast to considerably lower values of f_p by direct measurements of others. For example, Fricke (1990) finds values between 0.45 and 0.65 and Bratten (1989), found values in the vicinity of 0.5. Specific reasons for these differences are not known.

A model for pedestrian throw distance has been developed and presented. It contains what is believed to be the most important parameters and physical variables that play a role in planar vehicle-pedestrian collisions. The model is presented in two forms. One determines the throw distance as a function of the vehicle speed, $s_p = f(v_{c0})$. The other is a reconstruction form where, $v_{c0} = f(s_p)$. Not all of the parameters in the model were measured, recorded and/or controlled in the experiments and so not all of them could be evaluated or examined from the data. Fitted values of launch angles ranged from roughly from 5˚ to 10˚ for wrap collisions, based both on reconstructed collisions and experiments with dummies. In general, using least-square parameter values in the model and least-square fitted values of f_{eq} in the index equation resulted in nearly identical curves. This implies that the index equation (Eq 13) does nearly as good a job of matching experiments as does the model. Although true, the model is based on physical principles and measurable variables. Compared to the index equation, the model has greater flexibility and greater potential. If/when more detailed data becomes available, the model should provide a more precise method for both analyzing and reconstructing pedestrian collisions. It was shown that fitting empirical equations can present the potential hazard of masking physical reality.

Finally, fitted values of the velocity ratio, α, of 1.2 and 1.3 resulted from the analysis of forward projection collisions. Corresponding to the value of $f_p = 0.8$, this range of α indicates that the pedestrian (based on experiments using dummies) rebounds from the front of the vehicle at a speed higher than the vehicle by 20% to 30%. Of course, the pedestrian's speed must be at least equal to the speed of the vehicle, otherwise the pedestrian would "pass through" the vehicle. On the other hand, values of α between 1.2 and 1.3 seem rather high. This could be due to a difference in the restitution between dummies and human pedestrians. Consequently, these results should be verified by future experiments.

ACKNOWLEDGMENT

The authors graciously acknowledge the generosity of Andrew Happer, Michael Araszewski, Amrit Toor, Robert Overgaard, and Ravinder Johal for supplying most of the experimental data used in this paper. Collecting and supplying the data allowed this paper's authors to accomplish much more toward the main goals of the paper.

This research was conducted while the principal author was on a sabbatical leave (1999-2000) from Hong Ik University, Choongnam, Korea.

CONTACT

Correspondence for this paper should be sent to R. M. Brach, Room 105 Hessert Center, Department of Aerospace and Mechanical Engineering, University of Notre Dame, Notre Dame, IN 46556-5684, USA; raymond.m.brach.1@nd.edu.

REFERENCES

Ashton, S. J. and Mackay, G. M., "Car Design for Pedestrian Injury Minimization." Proc. of the Seventh International Technical Conference on Experimental Safety Vehicles, U.S. DOT, Washington, D.C., 1979b, pp. 630; also SAE Paper 796057

Backaitis, Stanley H., Accident Reconstruction Technologies — pedestrians and Motorcycles in Automotive Collisions, SAE, PT-35, 1990

Bratten, T.A., "Development of a Tumble Number for Use in Accident Reconstruction" SAE Paper 890859, 1989

Brooks, D., Wiechel, J., Sens, M. and Guenther, D. A., "A comprehensive review of pedestrian impact reconstruction." SAE Paper 870605

Dettinger, J., "Methods of improving the reconstruction of pedestrian accidents: development differential, impact factor, longitudinal forward trajectory, position of glass splinters (in German). Verkehrsunfall und Fahrzeugtechnik, Dec. 1996, 324-330 and Jan. 1997, 25-30

Eubanks, J. J., *Pedestrian Accident Reconstruction*, Lawyers & Judges Publishing Company, Tucson, AZ, 1994

Evans, A. K. and Smith, R., "Vehicle speed calculation

from pedestrian throw distance." , Proc. Instn Mech Engrs, Part D, Vol. 213, No. D5, pp. 441-448, 1999

Fricke, L. B., *Traffic Accident Reconstruction*, Northwestern University Traffic Institute, Evanston, IL, 1990

Happer, A., Araszewski, M., Toor, A., Overgaard, R. and Johal, R., "Comprehensive Analysis Method for Vehicle/Pedestrian Collisions", SAE Paper 2000-01-0846, March 2000

Hill, G. S., "Calculations of vehicle speed from pedestrian throw." *Impact*, J. Inst. Traffic Accident Investigation, Spring 1994, pp. 18-20

Kallieris, D. and Schmidt, G., "New Aspects of Pedestrian Protection Loading and Injury Pattern in Simulated Pedestrian Accidents", SAE Paper 881725, 1988

Kramer, Martin, "Pedestrian vehicle accident simulation through dummy tests." Nineteenth Stapp Car Crash Conference; SAE Paper 751165, 1975

Kuhnel, A., "Vehicle-pedestrian collision experiments with the use of a moving dummy." Proc. of Eighteenth Conference of American Association of Automotive Medicine, Toronto, Sept. 1974, pp. 223-245

Limpert, R., *Motor Vehicle Accident Reconstruction and Cause Analysis*, 4th Ed., The Michie Company , 1994

Limpert, R., *Motor Vehicle Accident Reconstruction and Cause Analysis*, 4th Ed., The Michie Company , Suppl., 1998

Lucchini, E. and Weissner, R., "Differences Between the Kinematics and Loadings of Impacted Adults and Children; Results from Dummy Tests." Proc. of the Fifth International IRCOBI Conference on the Biomechanics of Impacts, Lyon, pp. 165-179. 1980

Moser, A., Steffan, H., Hoschopf, H. and Kasanicky, G., "Validation of the PC-Crash Pedestrian Model", SAE Paper 2000-01-0847, March 1999

Ravani, B. and Brougham, D.; Mason, R.T., "Pedestrian Post-Impact Kinematics and Injury Patterns", SAE Paper 811024, 1981

Russell, C. G., *Equations and Formulas for the Traffic Accident Investigator and Reconstructionist*, Lawyers & Judges Publishing, Tucson, AZ, undated

Schneider, H. and Beier, G., "Experiment and Accident: Comparison of Dummy Test Results and Real Pedestrian Accidents." SAE Paper 741177, 1974

Searle, J. A., "The Physics of Throw Distance in Accident Reconstruction." SAE Paper 930659, 1993

Severy, D. J., "Auto-pedestrian collision experiments", SAE Paper 660080, 1966

Stcherbatcheff, G., Tarriere, C., Duclos, P., Fayon, A., Got. C. and Patel, A., "Simulation of collisions between pedestrians and vehicles using adult and child dummies." SAE paper 751167, 1975

Sturtz, G., Suren, E. G., Gotzen, L., Behrens, S., Richter, K., "Biomechanics of real child pedestrian accidents." Twentieth Stapp Car Crash Conference; SAE Paper 760814, 1976

Sturtz, G. and Suren, E. G., "Kinematic of real pedestrian and two wheel rider accidents, and special aspects of the pedestrian accident." Proc. of IRCOBI Meeting on Biomechanics of Injury to Pedestrians, Cyclists and Motorcyclists, Amsterdam, 7-8 Sept. 1976

van Wijk, J., Wismans, J., Maltha, J., and Wittebrood, L., "MADYMO pedestrian simulations", SAE Paper 830060,1983

Wood, D. P., "Impact and Movement of Pedestrians in Frontal Collisions with Vehicles. *Proc. of the Institution of Mechanical Engineers*, Vol. 202, No. D2, pp. 101-110, 1988

Wood, D. P. and C. K. Simms, "Coefficient of friction in Pedestrian throw", *Impact*, No. 1, pp12-15, 2000

Wood, D. P. and C. K. Simms, "Vehicle Speed Calculation from Pedestrian Throw Distance", Communication, *Proceedings, Institute of Mechanical Engineers*, Vol 214, pt D, pp 462-469, 1999